Biosensors and Bioelectronics 24 (2009) 3412–3418

Contents lists available at ScienceDirect

Biosensors and Bioelectronics

journal homepage: www.elsevier.com/locate/bios

Real-time monitoring of the strand displacement amplification (SDA) of human cytomegalovirus by a new SDA-piezoelectric DNA sensor system

Qinghai Chen[a], Zhihen Bian[a], Ming Chen[a], Xing Hua[a], Chunyan Yao[a], Han Xia[a], Hong Kuang[a], Xue Zhang[a], Junfu Huang[a], Guoru Cai[b], Weiling Fu[a,*]

[a] *Laboratory, The Clinical Experimental Base of Biosensor and Microarray, and The Center of Molecule and Gene Diagnosis, Southwest Hospital, Third Military Medical University, Chongqing 400038, PR China*
[b] *The 26th Electronics Research Institute of National Information Industry Department, Chongqing 400060, PR China*

ARTICLE INFO

Article history:
Received 15 April 2009
Received in revised form 3 June 2009
Accepted 3 June 2009
Available online 10 June 2009

Keywords:
Piezoelectric sensor
Strand displacement amplification (SDA)
Dynamic real-time monitoring
Human cytomegalovirus (HCMV)

ABSTRACT

Nucleic acid amplification has long been used in biosensor technologies, such as DNA sensors, DNA chips and microarrays, due to its advantage of high sensitivity in detecting target DNA. However, dynamic monitoring of nucleic acid amplifications with traditional DNA sensors in real-time is difficult since a constant temperature must be maintained during detection. Thus, the piezoelectric sensor, one type of traditional DNA sensor, is not applicable in real-time monitoring PCR due to the dramatic change in temperature that occurs during reaction. In this study, we introduced strand displacement amplification (SDA), an well-developed nucleic acid amplification technique that can work under conditions of constant temperature, into the development of a novel piezoelectric sensor. Using the new SDA-piezoelectric DNA sensor, we designed a stable system for liquid-phase detection, in which the crystal oscillator plate was fixed by an easily adjustable screw-threaded clamping mechanism and successfully applied the new sensor system to real-time SDA monitoring of human cytomegalovirus (HCMV). This new technique overcomes the shortcomings of traditional DNA sensors in real-time monitoring of nucleic acid amplification. The technique has proved to be a markedly simplified procedure with a number of advantages, such as higher sensitivity, better time efficiency, and the ability of dynamic real-time detection.

1. Introduction

Traditional DNA sensors are distinctive because of their high sensitivity in detecting the hybridization between the DNA probe and target sequence. Today, most of the studies on DNA sensors are aimed at improving their sensitivity. For example, studies on electrochemical sensors with the principle of enzymatic discrimination are mainly focused on the signal amplification of the micro-amount hybridization (Itamar and Bilha, 2001; Lucarelli et al., 2004; Lai et al., 2006). However, these sensors are limited because no amplification effect occurs during the process. If nucleic acid amplification techniques such as PCR are applied to these highly sensitive DNA sensors, real-time detection sensitivity can be greatly improved.

Although PCR is one of the most mature and widely used techniques among traditional nucleic acid amplification methods, it is still difficult to apply in traditional DNA sensors because of the dramatic changes in temperature and viscosity of the fluid during reactions. To detect the DNA hybridization signal with a traditional DNA sensor, certain preconditions are necessary, such as a stable reaction environment (e.g., stability of temperature, pressure, fluid viscosity, etc.). In this respect, traditional DNA sensors involve an essentially static process, under constant conditions of temperature, pressure and viscosity. Therefore, it is hard to dynamically monitor nucleic acid amplifications in real-time with traditional DNA sensors because a constant temperature must be maintained during detection. Thus, the use of the complicated PCR process and the elaborate separation and purification procedures which are required to isolate the products before detection is needed if using traditional DNA sensors. Currently, to achieve higher sensitivity in the detection of the target DNA, nucleic acid amplification is essential before detection for the most commonly used technologies, such as DNA sensors, DNA chips and microarrays (Lucarelli et al., 2004; Lai et al., 2006; Minmin and Guo, 2007; Scheller et al., 2001). If a new technology could be developed to dynamically monitor nucleic acid amplification in real-time, a number of advantages could be achieved, such as higher sensitivity, less time consuming, dynamic real-time detection, and a markedly simplified procedure (e.g., there would be no need to purify and rehybridize the products after amplification).

The piezoelectric sensor, also called the quartz crystal microbalance (QCM), has become one of the highlights in the biosensor research field due to its many advantages, such as its fast assay

* Corresponding author. Tel.: +86 23 68754429; fax: +86 23 65460909.
E-mail address: fuweinin@yahoo.com.cn (W. Fu).

0956-5663/$ – see front matter © 2009 Elsevier B.V. All rights reserved.
doi:10.1016/j.bios.2009.06.012

and response times, its high sensitivity, and its overall simplicity (Chang et al., 2000; Leonard et al., 2003; Wang et al., 2006). The incisal angle of the crystal oscillator is the core of the piezoelectric sensor and decides the characteristics of the resonant frequency and temperature. In detection, the incisal angle is fixed and a constant temperature must be maintained during detection. Thus the piezoelectric sensor, one type of traditional DNA sensor, is not applicable in real-time monitoring PCR due to the dramatic change in temperature that occurs during reaction.

Strand displacement amplification (SDA) is a complicated process of denaturation, displacement, extension and amplification of DNA, which works under the condition of constant temperature (Monis and Giglio, 2006; Nycz et al., 1998; Schweitzer and Kingsmore, 2001; Walker et al., 1995; Seelig et al., 2006; Ginocchio, 2004; Vanrompay, 2000). The SDA process can be divided into two steps (Fig. 1a): formation of the amplicon from the nucleic acid for amplification and strand displacement amplification of the amplicon (Nycz et al., 1998; Ginocchio, 2004). SDA has certain advantages (Vanrompay, 2000): (1) thermal cyclers are not needed; and (2) single- or double-stranded DNA can be amplified, which makes SDA a useful technique in piezoelectric sensors. Therefore, the current study is directed to the development of a new SDA-piezoelectric DNA sensor (also called SDA-QCM) technique, which can monitor the nucleic acid amplification reaction in real-time (Fig. 1a). The instability of the resonant frequency of piezoelectric sensors is a major problem in its application to liquid-phase detection of biological reactions. To solve this problem, we invented a new type of piezoelectric quartz sensor with an adjustable screw-threaded clamping mechanism that is very different from the usual design. The new technique of adjustable frequency siting showed a high level of frequency stability, and as such, was employed as the critical technique for application in piezoelectric sensors during liquid-phase detection.

Human cytomegalovirus (HCMV) infection greatly jeopardizes the health of human beings, especially congenital infections, HIV infection and infection occurring during organ transplantation (Hegde et al., 2005; Tomasec et al., 2005; Streblow et al., 2007; Goodrum et al., 2002). In this study, we applied the new SDA-piezoelectric DNA sensor to real-time monitoring of the SDA reaction of HCMV and obtained some encouraging results.

2. Materials and methods

2.1. Three piezoelectric sensors (Fig. 1b)

(a) *The glue-attached style piezoelectric quartz sensor*. Printed circuit boards (PCBs) are used worldwide for their wear-resistance, corrosion-resistance, etc. (Li et al., 2007). In this study, a PCB was used as the wall material into which a hole was made and a circular fillister was chiseled around the base of the hole; a crystal oscillator was mounted at the bottom of the hole before

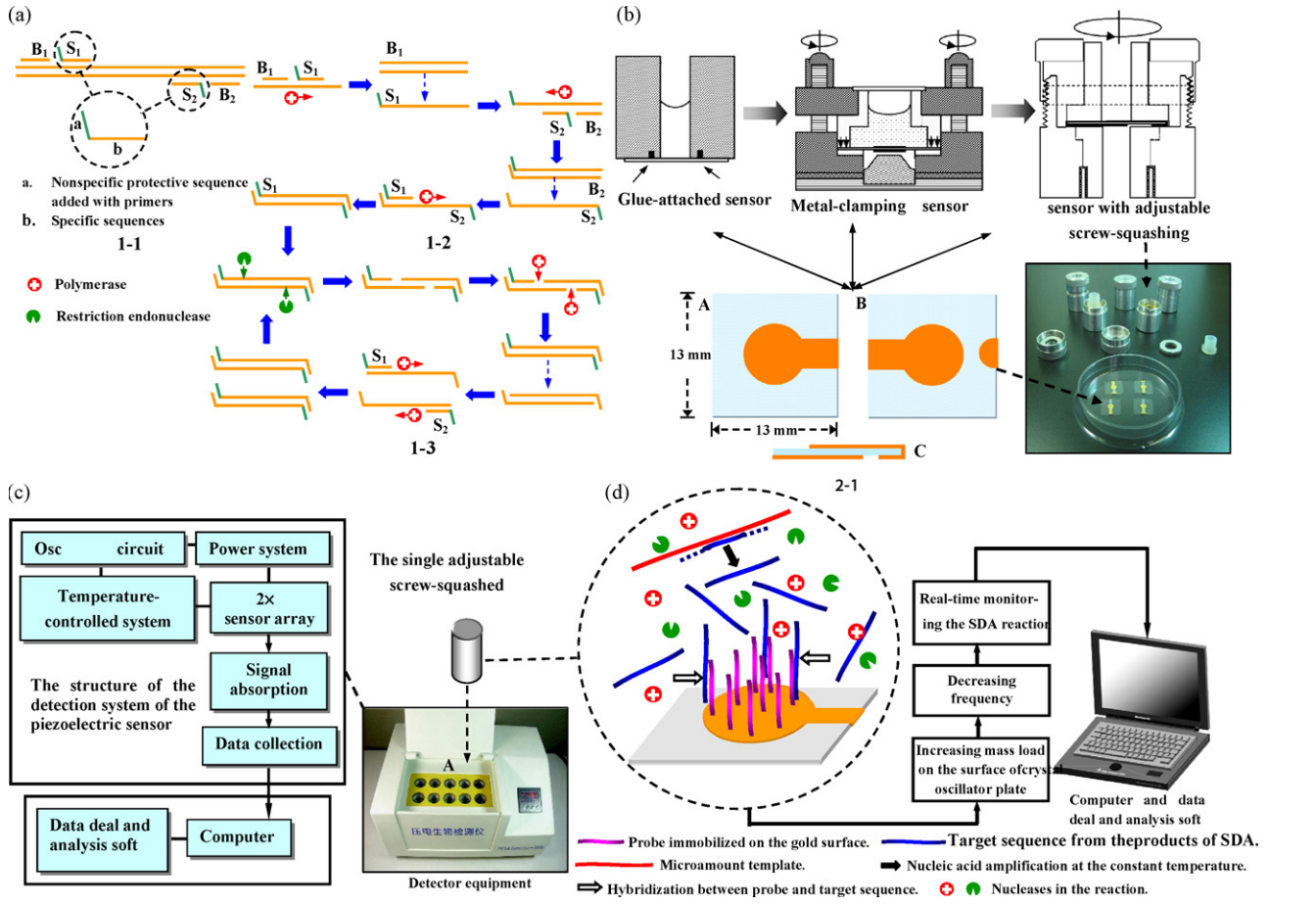

Fig. 1. Characteristic SDA-piezoelectric DNA sensor signatures are shown as follows: (a) Design of the SDA and its reaction. (1-1) Design of the primers; (1-2) Amplicons forming on the template; (1-3) Fast cyclic replication of amplicons. (b) The structure of the three piezoelectric quartz sensors and their crystal oscillator plates. (2-1) A crystal oscillator plate with curling gold films on both sides used in all of the above-mentioned sensors (A, front; B, back; C, side; the yellow zone represents the gold films and the blank zone represents the 10 MHz quartz AT-cut crystal); (2-2) Image of a piezoelectric quartz sensor with an adjustable screw-threaded clamping mechanism after being dismantled and a 13 mm × 13 mm square crystal oscillator plate with curling gold films. (c) Detection system of the piezoelectric quartz gene sensor. (A) The 2 × 5 array. (d) Principle of the immobilization of probes and the real-time monitoring of the SDA reaction on the sensors at constant temperature.

the fillister was gel-filled. (b) *The metal-clamping piezoelectric sensor*. The base modules of the stainless steel comprised upper and lower clamps, pressure nails and screws, side holders, a square pool hole, an emulsion sleeve, and a crystal oscillator plate, etc. (c) *The adjustable screw-threaded clamping sensor*. The sensor was composed of an adjustable screw cap, sliding holding columns, a cylindrical outer shell, an emulsion sleeve, a washer, electrode leaders, an electrode jack plug, a crystal oscillator plate, etc. Placing the emulsion sleeve on the crystal oscillator plate under the pressure of adjustable screw clamps constituted the detection pool. Both sides of the crystal oscillator plate were gold coated by ion sputtering subsequent titanium and gold films on the plate. A 13 mm × 13 mm square crystal oscillator plate was used as shown in Fig. 1b. The crystal oscillator plates used in the three sensors were fabricated from a 10 MHz quartz AT-cut crystal. The buffer solution was poured into the detection pools of the sensors, and their frequency changes were observed once the liquid surface had stabilized. Finally, the frequency stability of the three sensors was compared.

2.2. Sensor system and other instruments

The piezoelectric quartz sensor system comprised a detector (PESA-4000; Jialing Group of China) as shown in Fig. 1c. The adjustable screw-threaded clamping sensor, housing the crystal oscillator plate with gold films coated on both sides was inserted into the array ports on the host detector. During operation, the parameters (temperature, pathways and interval of frequency counting) were set. The real-time monitoring was conducted using frequency counting software.

2.3. Reagents

The primers: B_1: 5′-CGC TGA CGC ATT TGGA-3′; B_2: 5′-GCT CAG ACT ACA TGC CCTC-3′; S_1: 5′-CAA TTC CAC TCC AGA CTA CTC GGG CAG CGG CAG AAG AAG-3′; S_2: 5′-AGT GCA TCG AAT GTC TAT CTC GGG GCA ACG GGA GTT ACC-3′ were obtained from Shanghai Bio-Engineering Co. Probe DP_1 was sulfhydryl (SH), 5′-CAG CGG CAG AAG AAG-3′. Ps (primer hybrid) contained 0.5 μM B_1, 0.5 μM B_2, 1.0 μM S_1, 5.0 μM S_2. The SDA enzymes: BsoBI and exo-Bst DNA polymerase were obtained from New England Bio-labs, MA, USA. The HCMV type strain AD169 was obtained from the National Institute for the Control of Pharmaceutical and Biological Products. $MgCl_2$ and dNTP were obtained from Promega. BSA and DTT were obtained from Sigma. Tris, $MgCl_2{\cdot}6H_2O$, NaCl, K_2HPO_4, HCl, NaOH, absolute alcohol, heparin, and EDTA were all obtained from Shanghai Chemistry Reagent Co. 6-Hydroxide radical alcohol was obtained from Aldrich. All solutions were prepared using Ultrapure water (Milli-Q Plus system, Millipore) with a resistivity of 18.2 mho cm at 25°C.

2.4. SDA of HCMV

The following were added into the SDA reaction solution (50 μL in this case): Tris–HCl buffer (pH 7.9) 5 μL, 150 mM NaCl 5 μL, 100 mM $MgCl_2$ 5 μL, 1 g/L BSA 5 μL, 10 mM DTT 5 μL, 10 mM dNTP 10 μL, the primers (0.5 μM B_1 1 μL, 0.5 μM B_2 1 μL, 5.0 μM S_1 1 μL, 5.0 μM S_2 5 μL), and distilled water. Before use, 2 μL of the BsoBI enzyme and 1 μL of the Klenow enzyme were added to the solution and well mixed. Then, the target gene sample (the purified virus genome) was added to the mixture in preparation for reaction. The sample was heat denatured at a temperature of 94 °C for 5 min, rapidly cooled in an ice-bath to restore the solution to room temperature, and heated again prior to use (see Support information; Fig 1).

2.5. Immobilization of probes and real-time detection (Fig. 1d)

The gold films were immobilized on the crystal oscillator by using the self-assembled monolayer (SAM) technique with a suitable thiol compound (Carlisle and Layson, 2007; Schön et al., 2001). The electrode surface was first soaked and rinsed for 10 min in cleaning solution (30% H_2O_2:98% H_2SO_4 = 1:3) and then thoroughly washed with tri-distilled water and dried with pure nitrogen gas. Then, the DP_1 probe which was immersed in Tris–HCl buffer was immobilized and kept for more than 4 h at room temperature. The probes dissociating in the buffer were removed and the probe immobilized in on the gold film was treated with thioglycollic hexanol for 10 min. Then the probe was thoroughly rinsed with distilled water three times and dried with nitrogen gas before use. First, the crystal oscillator plate was inserted into the sensor, and the frequency adjusted until stable. Second, the reagent was then added to the detection pool and the frequency again adjusted until stable. Finally, the micro-amount target gene sample (the purified virus genome) was added in preparation for reaction. The sample was first heat denatured at a temperature of 94 °C for 5 min, then cooled rapidly in an ice-bath to restore the sample to room temperature, and finally heated again prior to use. The frequency counting card was set as 1 time/5 s and the frequency change was observed for more than 3 h.

3. Results and discussion

3.1. Comparison of frequency stabilities between the three piezoelectric sensors (Fig. 2)

The resonant frequency of the crystal oscillator plate can maintain stable for a long period in vapor, but is difficult to keep stable in the liquid-phase due to a variety of frequency-interrupting factors, which hampers the application of this sensor during liquid-phase detection (Uttenthaler et al., 2001; Rodriguez-Pardo et al., 2004; Vancura et al., 2007). The quality of the quartz crystal oscillator, a basic component of piezoelectric sensors, can be improved by certain processing techniques. The self-oscillating circuit is capable of maintaining good stability and strong oscillation in the liquid-phase. Detection cells are constructed by sealing the crystal oscillator plate and exterior materials inside the piezoelectric sensor and act as containers where the biological reaction takes place, which is critical for achieving frequency stability of the sensors in liquid-phase detection. In our study, we initially developed a glue-attached piezoelectric sensor, but it showed poor stability during liquid-phase detection (shift range ±15 Hz/h). Then, we turned to the metal-clamping piezoelectric sensor which showed a significant improvement in frequency stability with a shift range of ±1 Hz/h. However, it still showed certain disadvantages such as a complicated structure, complicated manipulation and poor practical application. In the end, we developed an adjustable screw-threaded clamping piezoelectric sensor which proved to be easy to operate as well as having good frequency stability with a shift range of ±2 Hz/h. during liquid-phase detection.

3.2. Adjustable piezoelectric sensor (Fig. 3)

The adjustable screw-threaded clamping piezoelectric sensor includes pressure and position adjusting, of which the former is predominant. The pressure adjustment works through the "pressure-frequency" relationship between the stress force on the crystal oscillator plate, the emulsion sleeve, the annuliform edge of the crystal oscillator plate and the resonant frequency of the sensor. The pressure adjustment is made by the intermittent mode, which allows simultaneous regulation and observation, and takes the scale

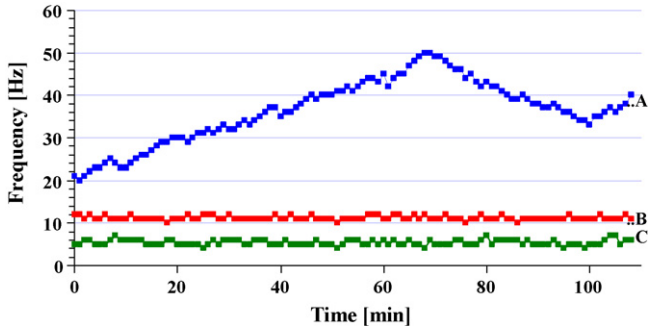

Fig. 2. Comparison of frequency stabilities between the three types of piezoelectric sensors during liquid-phase detection. (A) Glue-attached piezoelectric sensor; (B) Metal-clamping piezoelectric sensor; (C) Piezoelectric sensor with adjustable screw-threaded clamping mechanism.

at the edge of the hub and the pointer on the adjustable screw cap as the regulation location references. Of the two pressure adjustment methods available: i.e. "tightening then loosening" or "loosening then tightening", the former adjustment method is the most-widely used. However, if the first method fails, the second method can be employed with multiple adjustments until a stable fundamental frequency is obtained. Previously, the crystal oscillator plate was fixed in the piezoelectric sensor using molding fixation materials similar to those employed in the above-mentioned glue-attached method. However, it is very difficult to control the fine machining precision and even precision of the stress force on the annuliform edge so as to achieve an even distribution of the stress force on the annuliform edge. This is because the core of the piezoelectric sensor and the resonant frequency of the crystal oscillator plate are highly sensitive to the contact location of the annuliform fixation material, particularly around the detection cells. Therefore, screening of the molding fixation materials is increasingly being adopted. The technique of adjustable frequency siting can obtain rapid stabilization of the fundamental frequency by adjusting the crystal oscillator plate, and usually takes less than 5 min. The new adjustable piezoelectric sensor has several advantages, such as excellent fundamental frequency stability, simple operation, low cost, etc. The new sensor is a component which can be used alone or grouped together. The technique of *adjustable frequency siting* has shown a high level of frequency stability and can be employed as the critical technique in designing a stable platform for a piezoelectric sensor array for liquid-phase detection.

3.3. Basic reaction style and sample concentrations

Fig. 4 shows the frequency changes obtained during real-time monitoring of the reaction between SDA and HCMV at various sample concentrations with the SDA-piezoelectric sensor (see Support information; Table 1). The basic style of reaction is as follows: the left side of the figure shows the initial platform of the reaction before addition of the target gene sample. Then, the frequency shifted within a range of less than ±10 Hz for a period of time. After a while, the frequency shift showed an initial and slow decrease, followed by a short increase, before it finally decreased slowly, whereafter the frequency becomes steady. The whole process has been divided into three stages: *the incubating stage*, *the downward-shifting stage* and *the plateau stage*. No changes were observed for negative samples. The frequency difference analytical method of signal analysis was employed to judge the beginning and end points of the frequency response.

The piezoelectric quartz sensor can be categorized as a mass effect-based and non-mass effect-based type. Non-mass effect-based sensors which detect the change in viscosity and density of

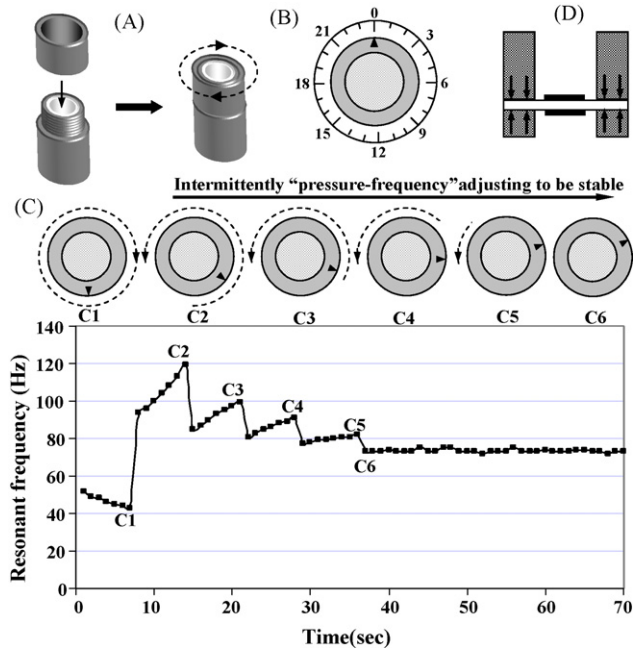

Fig. 3. Illustration of the principle of the piezoelectric sensor with an adjustable screw-threaded clamping mechanism. (A) Assembly of adjustable screw cap, sensor base and screw-threaded clamping mechanism. (B) The adjusting location references by the scale at the edge of the detector equipment array hub and the pointer on the adjustable screw. (C) The intermittent "pressure-frequency" adjusting mode. (C1) As the adjustable screw cap is turned tightly clockwise to increase the pressure, the frequency rises; (C2–C5) As the adjustable screw cap is turned anticlockwise to decrease the pressure; the frequency increase slows down gradually; (C6) As the fundamental frequency is adjusted to attain stability, the sensor reaches the operating state for use. (D) Stress force on the annuliform edge of the crystal oscillator plate.

a liquid have already been used in blood coagulation experiments (Shen et al., 2006; Lin et al., 2005), while mass effect-based sensors, which are more sensitive to the mass load, are more widely used and a more mature technology. The high sensitivity of the resonant frequency of the sensors to the changes of mass deposited on the surface of the crystal and the changes in the physical properties of the reaction substance such as viscosity, density and conductivity enable the sensors to detect mass changes at the nanogram level with a high degree of specificity (Shen et al., 2006; Wilson et al., 2007). The mass effect-based piezoelectric sensor meets the classic Sauerbrey relationship (Sauerbrey, 1959): $\Delta F = -2.26 \times 10^6 \Delta m f^2 / A$, where ΔF = frequency change in the oscillating crystal in Hz, Δm = the change of mass of the deposited film in g, f = the fre-

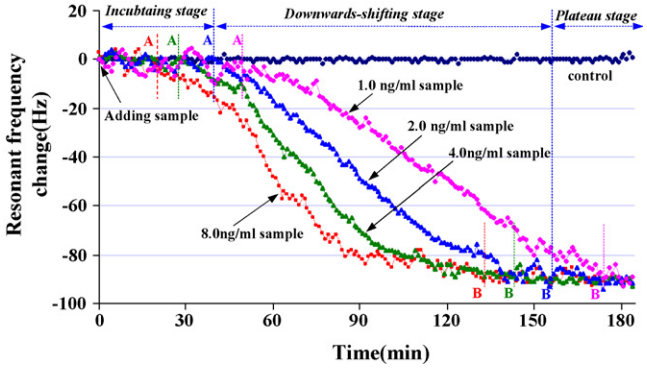

Fig. 4. Reaction mode of the SDA-piezoelectric sensor and the frequency changes when real-time monitoring the SDA of HCMV at various concentrations with the sensor. (A) End points of the incubating stage at various concentrations; (B) End points of the downward-shifting stage at various concentrations.

quency shift resulting from the change of mass, and A = the area of the electrode surface in cm^2; the minus sign represents the drop in frequency resulting from the weight increase of mass deposited on the surface of the sensors.

The reaction process of SDA, which is a complicated physical and chemical process, might affect the frequency shifting period prior to the decrease in frequency. The reaction was triggered by the target gene sample. An enormous number of target nucleic acid chains capable of binding to probes immobilized on the gold films of the sensors were generated by the denaturation, displacement, extension and amplification of DNA. Though the mass load would decrease the frequency, biomacromolecules such as enzymes and nucleic acids in the SDA system are expected to undergo sudden movement such as mass transfer and exchange, which would result in a dramatic change in the density and viscosity of the reaction mixture. The resonant frequency of the piezoelectric sensor was not only sensitive to the mass shift on the surface of the quartz plate but also highly sensitive to the changes in the properties of the reaction liquid such as the density, viscosity (Scheller et al., 2001; Lin et al., 2005; Wilson et al., 2007) and conductivity; the so-called the non-mass effects.

In fact, both the mass effects and non-mass effects of the piezoelectric sensors coexist. The frequency decrease based on the mass effects in the early stage of the reaction were slight and not sufficient to affect the frequency shift based on the non-mass effects, thus there existed a period of frequency shift, i.e., the *incubating stage*. Only when the reaction had lasted for a certain time and sufficient target nucleic acid chains had been generated to maintain the steady frequency drop of the sensor, that is, when the mass response was larger than the non-mass response, did the steady decrease of the frequency begin, i.e., the *downward-shifting stage*. When the frequency had decreased to an extent that the probes were consumed, this resulted in the *plateau stage*.

For the *incubating stage*, the length of time was dependent on the amount of target gene sample used. When the concentrations of sample were 8 ng/mL, 4 ng/mL, 2 ng/mL, and 1 ng/mL, the corresponding times of the *incubating stage* lasted for 20 ± 3 min, 29 ± 6 min, 39 ± 5 min, and 52 ± 11 min, and the *plateau stage* began at 129 ± 11 min, 141 ± 15 min, 164 ± 16 min and 172 ± 18 min, respectively. These results indicate that the shorter the *incubating stage*, the earlier the *plateau stage* begins. The frequency decrease values at the different concentrations of sample were practically identical (about 92 ± 3 Hz). The reason for this was probably because the total number of DP_1 probes immobilized on the gold film of the sensors was similar in the reaction, and the binding of all of the immobilized probes with the target nucleic acid chains became saturated so that the excess chains generated were unable to bind with the remaining DP_1 probes, resulting in a decrease in the resonant frequency caused by the mass response. At that time, the mass response of the sensors tended to cease and the frequency decreased slowly. However, the reaction of SDA did not end and the density and viscosity of the reaction liquid remained, so that the non-mass effect-based frequency shift continued to last more than 3 h (Walker et al., 1995). During the whole reaction process, the non-mass effects caused by the changes in the density and viscosity of the reaction liquid remained strong throughout the reaction, thereby interrupting the real-time monitoring of the SDA. Therefore, the curve of the frequency change was not as smooth as that in the static liquid-phase and the long-term shift of the frequency curve was significant.

3.4. Effect of different probe concentrations

Fig. 5 illustrates the frequency changes of real-time detection of the SDA, with the probes immobilized in different concentrations in the piezoelectric sensors (see Support information; Table 2). After the same amount of target DNA samples had been added to the detection pool of the sensors immobilized with probes of different concentrations, the reaction process was triggered and the incubation stage began. Because there was no difference in the amount of target gene sample added in the SDA process and the speed of the target nucleic acid chains generated remained the same, the incubating stage for the frequency shift of the sensors with the probes immobilized in the five different concentrations practically remained the same. This is despite the fact that the number of probes immobilized on the surface of the sensors varied. The reason for this was that the number of probes was far greater than that of the target nucleic acid chains generated in the early stage of the frequency decrease, such that the mass-frequency effects of the sensors decreased gradually and the downward-shifting stage ceased, thereby leading to the plateau stage. The magnitude of the frequency decrease and the time that the plateau stage began depended on the number of immobilized probes. As the immobilized probe concentration increased from 2 μg/mL to 4 μg/mL, the frequency correspondingly increased by 20 Hz (from 23 ± 2 Hz to 49 ± 6 Hz) or more. However, as the probe concentration continued to increase, the frequency decreased. That is, the $\Delta f/\Delta$probe concentration decreased with the increase in immobilized probe concentration. This inconsistency may result from the saturation of the probe sites on the gold film surface of the sensor when the immobilized probe concentration increased to a certain level. Thus, a further increase in the probe concentration in the solution did not lead to a corresponding significant increase in the number of probe sites, and the mass-frequency effect also tended to be saturated and did not rise further. Therefore, the $\Delta f/\Delta$probe concentration showed a linear decrease, rather than a non-linear decrease (see Support information; Fig 2).

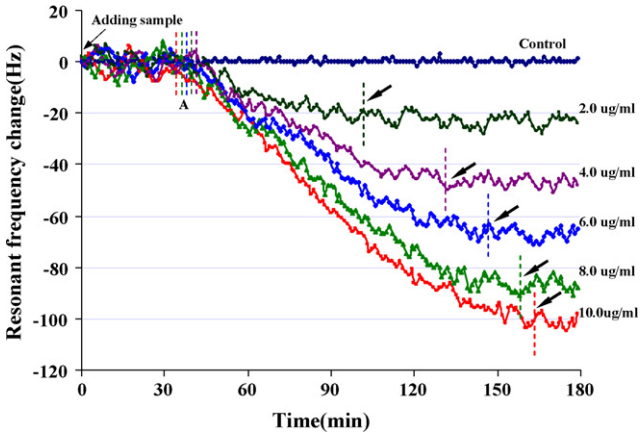

Fig. 5. Frequency changes of real-time detection of the SDA with the SDA-piezoelectric sensor at different probe concentrations. (A) End point of the incubating stage of SDA at different concentrations of the probe. Arrows: end point of the downward-shifting stage at different concentrations.

3.5. Effect of temperature

The frequency changes of the real-time detection in SDA at various temperatures are shown in Fig. 6 (see Support information; Table 3). A constant temperature reaction is the most important factor for SDA. The structure of the nucleases in the reaction polymerases and restriction enzymes is highly influenced by temperature. There is a great difference between the activities at different temperatures (Lage et al., 2003; Tonde et al., 2006; Kuettner et al., 2006). The nucleases at 52 °C might be slightly more active than those at 37 °C in the physiological condition. In this reaction, with the *incubating stage* at 52 °C, the reaction time was shortened compared with that at the reaction temperature of

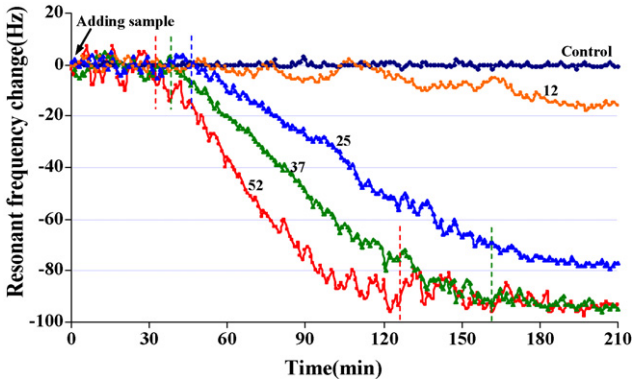

Fig. 6. Frequency changes of real-time detection of SDA at different temperatures.

37 °C (29 ± 5 min and 38 ± 6 min); the time of the *downward-shifting stage* at the reaction temperature of 52 °C was also highly sensitive to the change in temperature (Salavati et al., 2002; Lage et al., 2003) and was shorter than at 37 °C (127 ± 11 min and 162 ± 12 min, respectively). During the whole process (including the *downward-shifting stage*), the frequency shift at 52 °C was greater than at 37 °C, which might result from the fact that the reaction in the solution at 52 °C was more intense and caused a more marked non-mass response. After 170 min, the frequency shift seemed to decrease, which may result from the gradual consumption of the probes. However, the frequency decreases of the sensors at 52 °C and 37 °C (93 ± 4 Hz and 94 ± 5 Hz, respectively) were similar due to the consistency of the probe quantity immobilized on the surface of the gold films. The frequency response was still significant at 25 °C, while the incubating stage was prolonged slightly (46 ± 8 min), which indicated that, although less than at 52 °C and 37 °C, the nucleases maintained some activity at 25 °C. And, at that temperature, the sensor frequency stopped decreasing and tended to be steady after 190 min. This was attributed to the tendency of SDA to cease because of exhaustion of the various materials as the reaction time exceeded 3 h. Therefore, the sensor frequency shift at 25 °C (78 ± 6 Hz) was less than the corresponding frequency at 52 °C and 37 °C, although the consumption of the probes was not yet saturated. Because the processes of SDA at 25 °C and 12 °C had not been completed, the time calculation and end point estimation of the three stages were not fulfilled. The frequency change caused by SDA showed a slow fluctuation and a slight decrease at 12 °C. A great difference in the secondary structure of the ribozyme was observed at 12 °C and at 37 °C under physiological conditions (Tonde et al., 2006; Etchian and Pellerin, 2003). As the functional performance of the ribozyme depended on its space conformation, the activity of the ribozyme was extremely weak when it was below 12 °C.

4. Conclusion

The glue-attached piezoelectric sensor showed poor stability during liquid-phase detection. On the other hand, while the metal-clamping type sensor showed good stability during liquid-phase detection, it had the disadvantages of complicated manipulation and poor practicality. The adjustable screw-threaded clamping piezoelectric sensor evolved from the clamped sensor type was easy to handle and exhibited good frequency stability during liquid-phase detection. Our technique of *adjustable frequency siting*, which was used as the critical technique in designing this novel type of sensor, solved the problem of frequency instability of the sensors in liquid-phase detection.

The SDA reaction is a nucleic acid amplification technology under constant temperature condition, which can be employed in piezoelectric sensors. The basic model of frequency response of piezoelectric sensors used in SDA falls into three stages: the *incubating stage*, the *downward-shifting stage* and *the plateau stage.* The lengths of the three stages and the decrease in frequency are affected by the constant reaction temperature and the densities of the target genes and probes immobilized on the gold film surface of the sensors. The successive SDA reaction is a dynamic process and the none-mass effects caused by the changes in the viscosity and density of the liquid are strong and last continuously, thereby affecting the real-time monitoring of the SDA reaction with piezoelectric sensors. Therefore, the curve of frequency changes is not as smooth as that in the static liquid-phase and the long-time shift of the frequency curve is marked. The combination of a piezoelectric sensor with SDA resulted in a detection system capable of achieving real-time monitoring of nucleic acid amplification at constant temperature. This detection system shows many advantages, such as high sensitivity, less time consuming and dynamic real-time detection.

Acknowledgments

The research was supported by the Special Foundation for Scientific Instruments of the National 863 Project of P.R. China, the National Natural Science Foundation of P.R. China (30571775), the 11th 5-year Project of the Army (06G073) and Chongqing Family Planning Fund (2008-5).

Appendix A. Supplementary data

Supplementary data associated with this article can be found, in the online version, at doi:10.1016/j.bios.2009.06.012.

References

Carlisle, J., Layson, A., 2007. Electrochimica Acta 53, 1628–1634.
Chang, S.M., Hiroshi, M., Chikashi, N., Jun, M., 2000. Materials Science and Engineering C 12, 111–123.
Etchian, O.A., Pellerin, J.P., 2003. Comparative Biochemistry and Physiology Part B 134, 615–629.
Ginocchio, C.C., 2004. Clinical Microbiology Newsletter 26, 129–136.
Goodrum, F.D., Jordan, C.T., High, K., Shenk, T., 2002. Proceedings of the National Academy of Science of the USA 99, 16255–16260.
Hegde, N.R., Dunn, C., Lewinsohn, D.M., Jarvis, M.A., Nelson, J.A., et al., 2005. Journal of Cell Biology 171, 1109–1119.
Itamar, W., Bilha, W., 2001. Trends in Bio-technology 196, 222–230.
Kuettner, E.B., Pfeifer, S., Keim, A., Greiner-Stöffele, T., Sträter, N., 2006. Acta Crystallographica Section F Structural Biology and Crystallization Communications 62, 1290–1293.
Lage, J.M., Leamon, J.H., Pejovic, T., et al., 2003. Genome Research 13, 294–307.
Lai, R.Y., Lagally, E.T., Lee, S.H., Soh, H.T., Plaxco, K.W., Heeger, A.J., 2006. Proceedings of the National Academy of Science of the USA 103, 4017–4021.
Leonard, P., Hearty, S., Brennan, J., Dunne, L., Quinn, J., et al., 2003. Enzyme and Microbial Technology 32, 3–13.
Li, J., Xu, Z., Zhou, Y., 2007. Journal of Electrostatics 65, 233–238.
Lin, T.M., Cheng, T.J., Wu, T.H., Chang, H.C., 2005. Sensors and Actuators B 109, 270–277.
Lucarelli, F., Marrazza, G.M., Turner, A.P.F., Mascini, M., 2004. Biosensors and Bioelectronics 19, 515–530.
Minmin, L., Guo, L.H., 2007. Environmental Science and Technology 41, 658–664.
Monis, P.T., Giglio, S., 2006. Infection, Genetics and Evolution 6, 2–12.
Nycz, C.M., Dean, C.H., Haaland, P.D., Spargo, C.A., Walker, G.T., 1998. Analytical Biochemistry 259, 226–234.
Rodriguez-Pardo, L., Fariña, J., Gabrielli, C., Perrot, H., Brendel, R., 2004. Sensors and Actuators B 103, 318–324.
Salavati, R., Panigrahi, A.K., Morach, B., Palazzo, S.S., Igo Jr., R.P., et al., 2002. Molecular & Biochemical Parasitology 120, 23–31.
Sauerbrey, G., 1959. Zeitschrift für Physik 155, 206–222.
Scheller, F.W., Wollenberger, U., Warsinke, A., Lisdat, F., 2001. Current Opinion in Biotechnology 12, 35–40.
Schön, J.H., Meng, H., Bao, Z., 2001. Nature 413, 713–716.
Schweitzer, B., Kingsmore, S., 2001. Current Opinion in Biotechnology 12, 21–27.
Seelig, G., Soloveichik, D., Zhang, D.Y., Winfree, E., 2006. Science 5805, 1585–1588.
Shen, D., Zhang, H., Kang, Q., Zang, H., Yuan, D., 2006. Sensors and Actuators B 119, 99–104.

Streblow, D.N., Orloff, S.L., Jay, A.N., 2007. Current Opinion in Immunology 19, 577–582.
Tomasec, P., Wang, E.C., Davison, A.J., Vojtesek, B., Armstrong, M., et al., 2005. Nature Immunology 6, 181–188.
Tonde, S.S., Kumbhar, A.S., Padhye, S.B., Butcher, R.J., 2006. Journal of Inorganic Biochemistry 100, 51–57.
Uttenthaler, E., Schraml, M., Mandel, J., Drost, S., 2001. Biosensors & Bioelectronics 16, 735–743.
Vancura, C., Li, Y., Lichtenberg, J., Kirstein, K.U., Hierlemann, A., et al., 2007. Analytical Chemistry 79, 1646–1654.
Vanrompay, D., 2000. Seminars in Avian and Exotic Pet Medicine 19, 2–13.
Walker, G.T., Nadeau, J.G., Linn, C.P., 1995. Molecular and Cellular Probes 9, 399–403.
Wang, X., Zhou, J., Song, J., Liu, J., Xu, N., Wang, Z.L., 2006. Nano Letters 6, 2768–2772.
Wilson, T.L., Campbell, G.A., Mutharasan, R., 2007. Sensors and Actuators A 138, 44–51.